# Preliminary study of Behind Helmet Blunt Trauma Assessment using a Numerical Head Model

**N. Nsiampa**[1], F. Coghe[1]

[1] *Royal Military Academy, Renaissancelaan 30, Brussels 1000, Belgium*
nestor.nsiampa@dymasec.be

**Abstract.** Modern combat helmets, made of flexible composite materials with high ballistic performance and low weight, have significantly improved both ballistic protection and ergonomic comfort for soldiers. However, these lightweight helmets have a drawback: upon impact, they exhibit increased backface deformation, which raises the risk of blunt trauma injury, also known as Behind Helmet Blunt Trauma. Such injuries can impair a soldier's performance and, in severe cases, pose a threat to his/her life.
The study of the injury mechanisms associated with the Behind Helmet Blunt Trauma is challenging due to the highly dynamic and complex nature of ballistic impact events. To investigate this type of trauma, we used a finite element head model, originally developed for non-lethal impact applications. For this purpose, we replicated the experiments conducted by Freitas using a numerical approach. Due to the limitations in the modeling approach, only a qualitative analysis was performed. The preliminary results indicate that the model offers valuable insight into the impact dynamics. The role of helmet pads in mitigating injury is highlighted with off-pad impacts showing a notably higher risk of cranial injury compared to on-pad impacts. This trend is consistent with the experimental findings reported by Freitas.

## 1. INTRODUCTION

Most modern helmets are made of aramid material or of Ultra-High Molecular Weight Polyethylene (UHMWPE) material. These new composite flexible materials have improved soldier protection against fragments and small caliber rounds, and as well as comfort. However, they have also increased the risk of Behind Helmet Blunt Trauma (BHBT) due to an increase of helmet back face deformation (BFD), which may impair the soldier's performance and even endanger his/her life.

BHBT is a type of blunt trauma characterized by an induced non-penetrating injury to the head caused by helmet impact-related events. A ballistic impact on a helmeted soldier can be divided into two impact phases: a primary impact caused by the interaction between the threat and the helmet shell and a secondary impact between the helmet dynamic BFD and the head. The former impact can be considered as a high speed and low mass impact and the latter as a lower speed and slightly higher mass [1,2]. Therefore, the strain rates generated during the initial bullet-helmet impacts are higher than those induced by the helmet's BFD on the head.

Numerous studies have been conducted, particularly in the civilian world, to better understand the injury mechanisms associated with blunt impacts characterized by lower rate loadings and develop safety equipment such as helmets in order to ensure the protection and safety of people and reduce severe or fatal injuries in road, sports, automotive and workplace accidents [3-7]. For ballistic impact events characterized by high rate loadings, only a few studies have investigated this type of impacts and the resulting injuries. Tests on human beings are ethically unacceptable, so mechanical or biological surrogates are used to provide baseline biomechanical response, to investigate BHBT injury and injury tolerance levels and to assess the risk of injury associated to such events [8-12]. Unfortunately, there is still a lack of standardized procedures for testing methods, clear injury criteria, and injury tolerance levels for injury assessment.

Today, with the development of computing techniques, finite element (FE) models offer an additional alternative method [12-16]. However, there are still multiple challenges to overcome. On the one hand, anthropometric human body FE models are built with great levels of anatomical details, but the validation is still incomplete because biomechanical test data are generally complicated and expensive to obtain. On the other hand, material models that describe the model response under high rate strain loadings require dynamic characterization experiments in order to obtain the model parameters. However, this is not straightforward due to the anisotropic behavior of human tissues and the short time scale involved.

In the context of performing BHBT risk assessment using numerical simulations, an in-house 50$^{th}$ percentile finite element head model, originally developed for kinetic energy non-lethal applications, is used to investigate to which extent this model can also be implemented for BHBT applications. This preliminary study aims to compare the results of the head model's results with experimental data

https://doi.org/10.52202/081621-0013

reported in Freitas'paper [11]. The present study is limited to the impact of a 9x19mm Full Metal Jacket (FMJ) projectile on a helmeted head under frontal 0° NATO impact conditions.

The next sections give an overview of Freitas' experiments and a brief summary of head injury criteria.

### 1.1 Freitas experiments

Freitas et al. conducted non-perforating ballistic tests using various projectile types on a helmeted Human Head Surrogate (HHS) to gain insights into injury mechanisms within the scope of BHBT studies [11]. The HHS was composed of refreshed human craniums, a cerebral spinal fluid (CSF) surrogate, and soft tissue surrogates representing the skin, dura, and brain. Perma-gel was used to simulate the skin and was molded to the cranium, while the brain surrogate consisted of a mixture of perma-gel and iron powder. The CSF surrogate was water pressurized to 2 MPa, and the dura surrogate was modeled as a thick layer of silicone. The head surrogate was supported by a Hybrid III 50th Male Neck assembly.

The helmet used for the tests was the US Marine Corps' large-sized Lightweight Combat Helmet (LWH). This helmet is made of a para-aramid shell, and a pad system and a suspension system [17-18]. The protection system for lower energy projectiles consisted of the helmet only. For higher energy projectiles, the protection system consisted of the helmet with a ceramic applique layup. The pad system consisted of 7 paired sets of hard and soft pads that were distributed as follows: one crown pad set, four lateral pad sets, and one front and one back pad sets. Two different pad systems configurations were used. The 7-pad configuration consisted of paired pads located at the front center, front right, front left, back center, back right, back left, and on the crown and the 5-pad configuration was derived from the 7-pad configuration where the front and the back center paired pads were removed. Two types of frontal impacts were considered: the front on-pad impacts for the 7-pad configuration and the front off-pad impact (no pad support on the impact location) for the 5-pad configuration.

On-pad impacts with 9x19 mm FMJ bullets resulted in lower intracranial pressures and skull strains and consequently, reduced likelihood of injuries when compared with the off-pad impacts. The authors concluded that in general, the pads provided an effective energy dissipation mechanism that helped to mitigate injury. Moderate skull fractures were observed for front center off-pad impacts while there was no injury or cranial fracture for on-pad impacts. The mean peak intracranial pressure and the mean peak strain value they reported for the occurrence of moderate cranial fracture was 255 kPa and of -0.21% respectively.

### 1.2 Injury criterion

A variety of head injury criteria are referenced in the literature for assessing head trauma. Generally, the type and severity of blunt impact injuries depend on the rate and magnitude of the impact load, as well as the specific region of the body affected. The main head injuries are skull fracture, skin lacerations or contusions, concussion, hemorrhaging, hematoma (blood clots), anoxic injury (lack of oxygen), and diffuse axonal injury (DAI) which is a damage to the brain neurons [19].

The injury can be mild, severe, or even fatal. A variety of physical parameters are used to predict head lesions: the maximum head force, the intracranial pressure (ICP), the head accelerations (linear or rotational), the strain, the stress and the energy. A review of injury criteria can be found in [20,21].
It is worth mentioning that there is still a lack of standardized procedures for testing methods, clear injury criteria, and injury tolerance levels for injury assessment from ballistic impacts. For example, Table I gives tolerance values found in literature for the occurrence of skull injury for blunt impacts relative to intracranial and peak maximum principal strain.

**Table 1.** Reported skull fracture tolerances

| **Skull fracture** | | | |
|---|---|---|---|
| ***Injury criterion*** | ***Tolerance*** | ***Risk of injury*** | ***Refs.*** |
| | | | |
| **Intracranial pressure** | | | |
| | 51.2 kPa | 50% skull injury | [22] |
| | 560 kPa | 50% risk of severe fracture injury | [23] |
| | 150 kPa | Significant risk of fracture | [24] |
| | 255 kPa | Moderate cranial injury | [11] |
| **Peak maximum principal Strain** | | | |
| | -0.5 % | 50% skull injury | [25,26] |
| | -0.4 % | Fracture | [11] |


https://doi.org/10.52202/081621-0013

## 2. METHODOLOGY

To gain deeper insights into BHBT and assess the associated injury risks, a finite element model of a human head protected with a combat helmet was used to perform ballistic impact simulations using 9x19 mm FMJ bullets. The 50$^{th}$ percentile head model was developed within the framework of injury risk assessment for kinetic energy non-lethal impacts and the validation is presented in Section 3.2. The aramid helmet shell model was developed and validated against experimental ballistic tests on BFD in [27]. The material properties of the 9 x19 mm FMJ bullet were retrieved from [28]. Section 3.3 presents the validation of the foam pads of the helmet.

The setup of the impact of 9x19 mm FMJ on the protected head was similar to the experiment one with two configurations, the 7-pad configuration and the 5-pad configuration (see section 1.1). No head support was modeled. Two types of impacts were considered as in the experiments: the on-pad impact and the off-pad impact. Only frontal normal (0° NATO) impacts were considered in this study. All the simulations were performed with LS-Dyna software [29].

To assess the risk of skull fracture, intracranial pressure and cranial strain were used as injury criteria and to compare the numerical results with those from Freitas' experiments, intracranial pressure was measured within the CSF and the cranial strain was measured in the skull at the same location as in the experiments.

## 3. FE modelling

### 3.1 Setup

Figure 1 shows the setup for the impact of 9x19 mm FMJ against a protected head. Experimental tests were carried out using large-sized aramid helmets while in the simulations, medium sized aramid helmets were considered to be consistent with the 50$^{th}$ percentile head model. Unlike the experiments, the numerical simulations did not include a suspension system. Additionally, unlike in the experiments where the head was supported by the Hybrid III neck assembly, the head was not supported and could move freely. Finally, material properties of the head soft tissues were also different from the experiments as the actual soft tissue material models defined in the 50th percentile model for non-lethal impacts were used (see section 3.2).

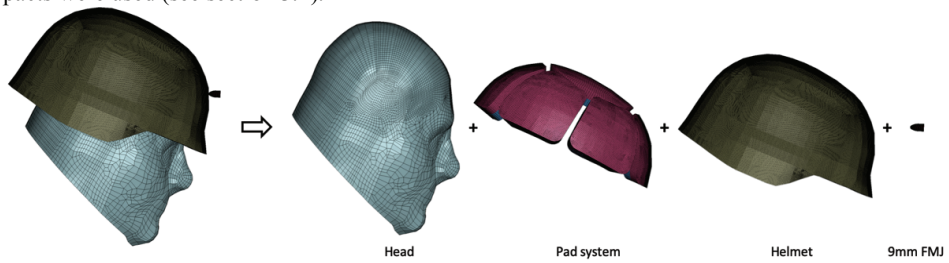


**Figure 1:** Setup of the impact of 9x19 mm against a protected head

Due to symmetry considerations, a half-model was used in the simulations. The analysis focused on two distinct helmet-only impact scenarios: (i) a frontal on-pad impact with the 7-pad configuration, and (ii) a frontal off-pad impact with the 5-pad configuration. Both cases involved normal (0° NATO) impacts using a 9 x19 mm FMJ projectile at a velocity of 435 m/s. Numerical sensors were placed within the CSF and the skull at the frontal impact site, matching the experimental setup, to record intracranial pressure and strain time histories. The next two sections briefly describe the validation of the head model and the foam models.

### 3.2 The head model validation

The 50$^{th}$ percentile head model developed in the framework of kinetic energy non-lethal applications was used in this study. Table 1 summarizes the different organs/tissues of the head that were modeled and the corresponding material properties. All the head organs except the CSF were modeled with linear elastic material models. A fluid-like material model was used for the CSF. It is important to note that no failure model was implemented in the current head model.

https://doi.org/10.52202/081621-0013

**Table 2.** Material properties of the head model

| Organ | Material model | ρ (g/mm^3) | E (MPa) | ν (-) | K (Mpa) | $G^0$ (Mpa) | $G^\infty$ (MPa) | β (ms^-1) | Refs. |
|---|---|---|---|---|---|---|---|---|---|
| Skull | Elastic | 2.00E-3 | 6000 | 0.21 | - | - | - | - | [30] |
| Falx Tentorium Meninges | Elastic | 1.14E-3 | 31.5 | 0.45 | - | - | - | - | [31] |
| Mandible Ethmoïd Face | Elastic | 2.00E-3 | 5000 | 0.23 | - | - | - | - | [31] |
| Scalp | Elastic | 1.24E-3 | 16.7 | 0.42 | - | - | - | - | [31] |
| Cerebrum Cerebellum Brainstem Callosum | Viscoelastic | 1.04E-3 | - | - | 1125 | 0.049 | 0.162 | 0.0162 | [31] |
| | | | | | | VC | | | |
| CSF | Fluid | 1.04E-3 | | | 2190 | 0.1 | | | [32] |

Where ρ is the material density, E, the Young modulus, ν, the Poisson's ratio, K, the bulk modulus, $G^0$ and $G^1$ are short-time shear modulus and infinite shear modulus, and VC, the viscous coefficient.

The head model was validated against the experimental data from low dynamic impact tests performed on cadavers by Yoganandan et al. [33] and Nahum et al. [34]. Figure 2 presents a comparison between the numerical and experimental results. In both cases, satisfactory agreement was achieved when predicting the impact force and intracranial pressure (ICP).

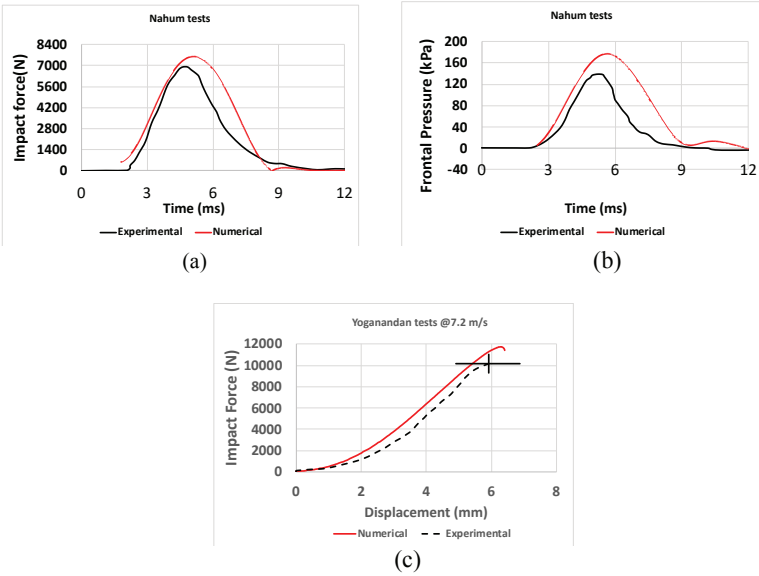


**Figure 2:** Head model validation: (a)-(b) Nahum tests[34]: Impact force and intracranial pressure ICP (c) Yoganandan tests [33]: impact force-displacement

### 3.3 The foam model validation

The helmet incorporated a foam pad system, consisting of a combination of hard foam and soft foam layers to optimize both energy absorption and wearer comfort. To validate the pad system, quasi-static tests performed in [35] are numerically replicated.

The quasi-static tests (Figure 3) involved a 5 kg-cylinder, representing a human head, impacting a bilayer foam pad composed of paired hard and soft foam pads wrapped in a water-resistant, airtight covering (not modelled in this study). Each foam pad had a diameter of 127 mm and a thickness of 9.5 mm. The foam pad materials were modeled using hyperelastic models, with compressive stress-strain curves at two different strain rates implemented as input curves for each foam type. (Figure 4). The impact velocities were 3.1 m/s and 4.3 m/s.


https://doi.org/10.52202/081621-0013

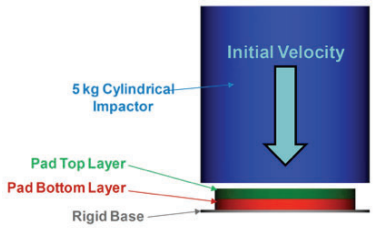


**Figure 3.** Experimental cylinder impact test setup [35]

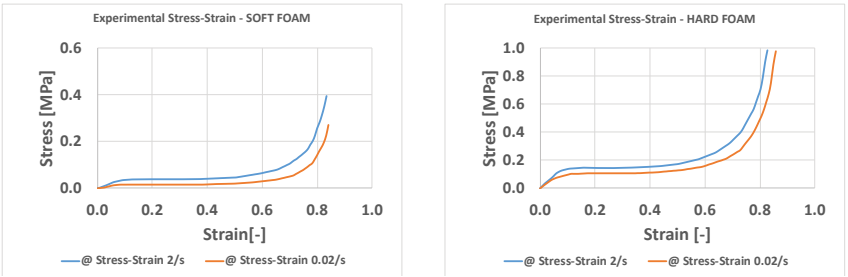


(a) (b)

**Figure 4.** Experimental stress-strain loading curves: (a) Soft foam - (b) Hard foam [35]

Comparison between numerical results and experimental results are given in Figure 5. The simulation results show good correspondence with the experimental data especially for the impact velocity of 3.1 m/s. The model overestimates the cylinder acceleration for the impact velocity of 4.3 m/s i.e. the material tends to exhibit an increased stiffness.

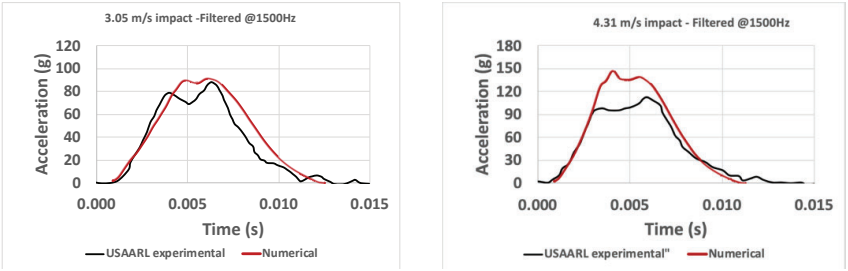


(a) (b)

**Figure 5.** Comparison between numerical and experimental results: (a) 3.1 m/s - (b) 4.3 m/s

## 4. SIMULATIONS

This section describes the results of the impact of 9mm FMJ bullet on the protected head.

### 4.1 Results

4.1.1 Seven-pad and five-pad configuration results

Figures 6(a) and 6(b) illustrate the evolution of intracranial (CSF) pressure and cranial strain at the impact site for both the 7-pad (on-pad) and 5-pad (off-pad) configurations. The intracranial pressure curves in Figure 6(a) exhibit high-frequency oscillations in both cases, with a noticeably greater damping effect observed in the on-pad configuration. This damping effect is further emphasized in the auto power spectrum (energy distribution) analysis of the two pressure signals shown in Figure 6(c). Additionally, Figure 7(d) presents the impact force curves for both configurations, revealing that the maximum impact force in the on-pad configuration is lower than that in the off-pad configuration.

https://doi.org/10.52202/081621-0013

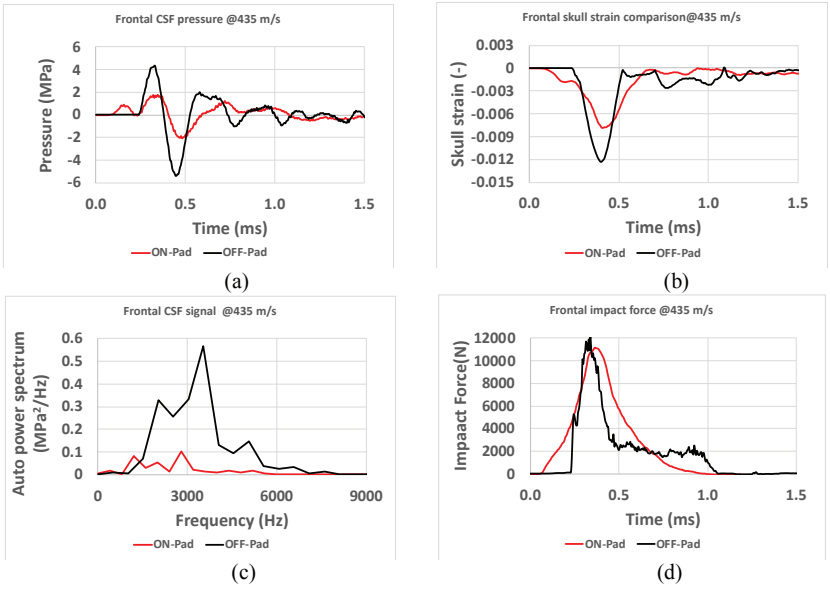


**Figure 6.** Numerical results corresponding to the 7-pad (on-pad impact) and 5-pad (off-pad impact) configurations at the impact zone.

A closer examination of the on-pad impact dynamics, especially during the loading phase shows how the energy is transferred and/or absorbed, contributing to a deeper understanding of head injury mechanisms. Figure 7 provides insight into the complex impact dynamics by illustrating the chronological evolution of the impact event within the impact zone. This evolution is effectively highlighted through the skull strain time history, which clearly delineates the distinct phases of the impact loading dynamics.

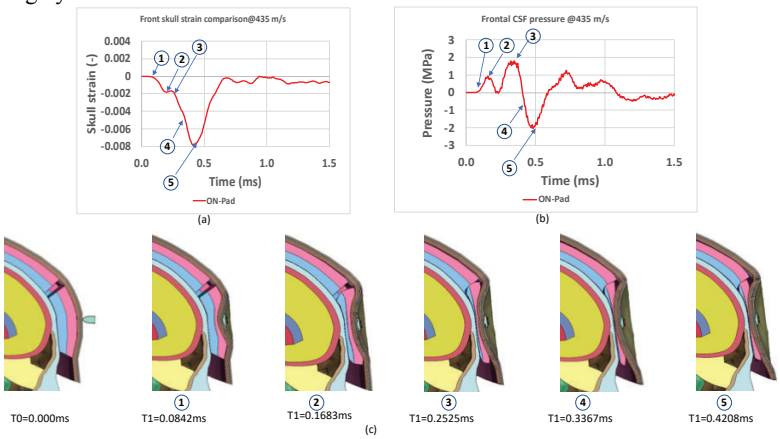


**Figure 7.** Different phases of the frontal impact dynamics

These distinct phases are globally characterized by the change in the slope of the strain time history, indicating a transition to another impact loading phase as observed in Figure 7(a) and Figure 7(c).

Up to point 1: The initial impact leads to the compression of the hard foam pad (pink color), the soft foam pad (blue color) is only slightly compressed;

Up to point 2: The soft foam pad is almost fully compressed under the loading of the hard foam and the helmet shell, but the skin (light blue color) is only slightly compressed;

Up to 3: Both foam pads continue to be compressed by the action of the helmet and act as a rigid body leading to a significant loading of the skin layer and the head;

Up to point 4: The skin layer becomes fully compressed under the loading of the protective system which continues to act as a rigid body;


https://doi.org/10.52202/081621-0013

Up to point 5: at this stage, the head has reached a full loading, and the unloading process begins. Beyond point 5, the unloading process continues.

After identifying these key points in the strain time history, corresponding points can also be identified in the pressure time history as shown in Figure 7(b).

4.1.2 Numerical vs experimental results for the 7-pad configuration

Figure 8 presents the numerical and experimental curves of the front CSF pressure and the front skull minimum principal strain within the impact location. There is a difference between the two curves of the two metrics in term of profile and value.

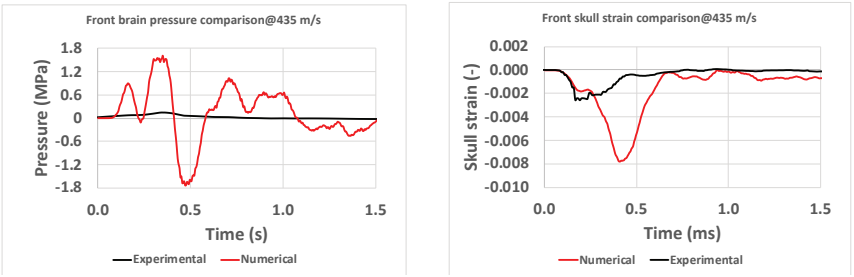


(a) (b)

**Figure 8.** Numerical and experimental results: (a) front pressure and (b) front skull minimal principal strain at the impact zone in the 7-pad (on-pad) configuration

**4.2 Discussions**

4.2.1 Comparison between the 7-pad and 5-pad configurations

Figures 6(a)-(c) show the differences in the head dynamic response associated with the 7-pad and 5-pad configurations. These differences are particularly highlighted in Figure 6(d) when we compare the impact force. Indeed, the on-pad impact results in a smoother mechanical loading of the head due to the cushioning effect of the pads (mainly the center pad), which gradually absorb and distribute the impact force. In contrast, the off-pad impact configuration, characterized by a lack of a front center padding leads to a more sudden and direct impact of the helmet shell backface to the head. This difference in loading mechanisms significantly affects the mechanical response of the head, as reflected in the variations in intracranial pressure and cranial strain observed between the two configurations. Moreover, the intracranial pressure of 4.2 MPa and the minimum principal strain of (-1.2%) for the off-pad impact are greater than the intracranial pressure of 1.9 MPa and the minimum principal strain of (-0.75%) for the on-pad impact, and similarly, the maximum impact force for the off-pad impact (12 kN) is greater than for the on-pad impact (11kN). These results indicate that there is a higher risk of skull fracture associated with the off-pad configuration than the on-pad configuration. A similar trend was observed in the experimental data.

The unloading process in Figure 6(d) differs between the two configurations. In the on-pad configuration, unloading is smooth and continuous. In contrast, the off-pad configuration shows an initial phase of quick unloading of the helmet shell followed by a plateau, during which the residual force exerted on the head remains nearly constant. This plateau may correspond to the ongoing relaxation of the pads. Finally, a terminal phase occurs where the force drops to zero, indicating that there is no more contact between the helmet backface and the head.

A frequency analysis using the auto power spectrum performed on the pressure time histories (Figure 7(c)) reveals a significant attenuation in amplitude (or energy) for the on-pad configuration, along with a leftward shift (towards lower frequencies) in the spectrum indicating a reduced frequency spectrum compared to the off-pad configuration. The on-pad configuration compared to the off-pad impact demonstrates a clear damping effect on high-frequency oscillations. This suggests that the pads effectively absorb and dissipate impact energy, thereby reducing the intensity of the interaction between the BFD and the head.

On the other hand, the head is a complex structure and the material properties of the head model play also a key role in the head dynamics as well as the wave reflections at different interfaces. Moreover, the intracranial content (brain, cerebellum …) constituted of soft tissues surrounded by the CSF (modelled as a fluid) may oscillate relative to the skull.

https://doi.org/10.52202/081621-0013

4.2.2 Comparison between the numerical and experimental results

Regarding skull injury severity in BHBT assessment, the maximum intracranial pressure and minimum principal strain values predicted by the numerical head model for both on-pad and off-pad impacts are significantly higher than the injury tolerance thresholds reported by Freitas et al. [11] and other values summarized in Table 1. This indicates that the numerical model may overestimate injury severity. However, this observation should be interpreted with caution regarding the actual occurrence of skull fracture injuries based solely on these results. The discrepancy likely stems from the fact that the numerical model does not fully replicate the dynamics of the experimental tests particularly because the helmet model was validated using data from helmets different than those in Freitas' experiments. This highlights the need for further investigation and refinement of the helmet material models to enhance the fidelity and predictive accuracy of the simulations assuming that material data for the specific type of LWH helmets used by Freitas can be obtained.

Aside from the helmet considerations, two additional factors may be investigated regarding the head model:

(i) The soft tissue models used in the head model may behave differently from the experimental soft tissue surrogates, as they were not validated against these surrogates.

(ii) The current numerical head model was initially developed for non-lethal impact applications, which may not be suitable for BHBT applications. Therefore, it may be necessary to further investigate and adapt the head model to improve its predictive capability for BHBT. This will require more biomechanical data specifically derived from ballistic tests.

In Section 4.1.1, key points were identified corresponding to the onset or transition between different phases of the impact loading process, as observed in both the strain and pressure time histories in Figure 7 and Figure 9(a). When these key points are compared to the experimental pressure time history, similar features can also be identified that delineate the distinct loading phases previously described (Figure 9(b). This similarity across the various impact phases suggests that the numerical model can qualitatively capture the characteristic impact dynamics observed in the experimental tests.

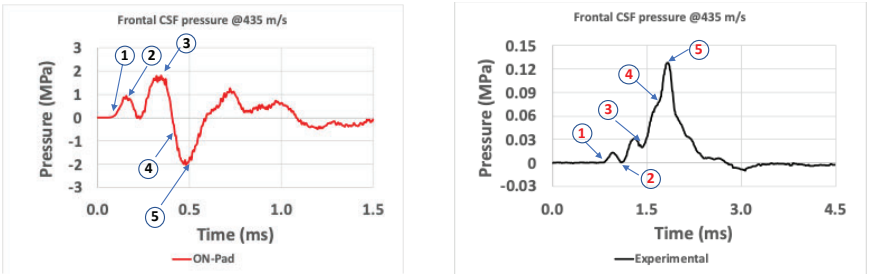


(a) (b)

**Figure 9.** Pressure histories -Idenfication of transition corresponding points of the impact phases: (a) Simulation – (b) Freitas' experiment [11]

4.2.3 Limitations

There are few limitations to our numerical approach. There was a difference in helmet material properties between the helmets consistent with the 50$^{th}$ percentile head model from which the material model used in our study was derived and the large sized helmets used in Freitas' experiments. Likewise, the head soft tissues material properties of the head model were different from those of the experimental surrogates which might not accurately reflect the mechanical response. Therefore, the impact dynamics may not have been correctly captured.

The pad model did not incorporate high strain rate dependency.

The numerical head was free to move while the HHS was fixed to the Hybrid III neck.

The finite element head model used was originally developed for non-lethal impact applications and might not fully capture the complex biomechanical response of head tissues under high-rate ballistic loading.


https://doi.org/10.52202/081621-0013

## 5. CONCLUSIONS

An in-house finite element model of the head, originally developed for non-lethal impact applications, was used within the BHBT framework to assess its applicability to BHBT scenarios. Freitas' experiments were replicated to see at which extent the head model could be used to investigate the BHBT and to gain a better understanding of the impact dynamics. The intracranial pressure and the cranial strain were used as metrics for cranial injury risk assessment.

The results showed that the model could qualitatively capture the main phases of the impact dynamics and provide valuable insight into the mechanical behavior observed during ballistic impacts. Key features which delineated the different phases of the loading process were identified that helped to better understand the impact dynamics. Similar features were also identified in the experiments.

A clear distinction was observed between the 7-pad (on-pad) and 5-pad (off-pad) impact configurations, with the off-pad impacts generating higher pressure, strain, and impact forces showing the role of the pads in dissipating the energy. Therefore, the model predicted a higher likelihood of cranial injury with the 5-pad configuration compared to the 7-pad configuration. A similar trend was observed in experiments.

When compared to the experimental tolerance thresholds, the numerical results consistently showed higher values for all the two metrics, indicating a risk of high predicted severity of cranial injury. However, this observation should be taken with cautious.

A further investigation to enhance the predictive capability of the head model by using additional ballistic biomechanical experiment or by incorporating strain rates dependent material models to see at which extent the model developed for non-lethal applications is suited for BHBT. Nevertheless, through this qualitative analysis, the model showed promising and potential capability for BHBT study.

## References


[1] Hisley, D. M., Gurganus, J. C., and Drysdale, A. W. (August 8, 2011). "Experimental Methodology Using Digital Image Correlation to Assess Ballistic Helmet Blunt Trauma." ASME. J. Appl. Mech. September 2011; 78(5): 051022. https://doi.org/10.1115/1.4004332

[2] Young L, Rule GT, Bocchieri RT, Walilko TJ, Burns JM, Ling G. When physics meets biology: low and high-velocity penetration, blunt impact, and blast injuries to the brain. Front Neurol. 2015 May 7;6:89. doi: 10.3389/fneur.2015.00089. PMID: 25999910; PMCID: PMC4423508.

[3] Determining Estimates of Lives and Costs Saved by Motorcycle Helmets, (NHTSA, March 2011. DOT HS 811 433, National Highway Traffic Safety Administration, Washington, DC), http://www-nrd.nhtsa.dot.gov/Pubs/811433.pdf

[4] Yang K.H., Hu J., White N.A., King A.I., Chou C.C., Prasad P., Development of numerical models for injury biomechanics research: a review of 50 years of publications in the Stapp Car Crash Conference. Stapp Car Crash J. (2006); 50:429-90. doi: 10.4271/2006-22-0017. PMID: 17311173.

[5] Global Status Report on Road Safety: Time for Action, WHO, (2009). The World Health Organization, Geneva, ISBN 9789241563840 https://iris.who.int/bitstream/handle/10665/44122/9789241563840_eng.pdf

[6] Abbas A.K., Hefny A.F., Abu-Zidan F.M., Does wearing helmets reduce motorcycle- related death? A global evaluation. Acct Anal Prev (2012) 49:249–252, doi:10.1016/j.aap.2011.09.033

[7] Snyder R.G.; Foust D.R.; Bowman B.M., Study of impact tolerance through free-fall investigations. Technical report (1977). Corporate Author: Highway Safety Research Institute, Ann Arbor, Mich, https://hdl.handle.net/2027.42/725

[8] Bass C., Bolduc M., and Waclawik S., Development of a Non-Penetrating, 9mm Ballistic Helmet Trauma Test Method. Proceedings of the Personal Armour Systems Symposium, (2002) pp. 18-22

[9] Raymond D.E. Biomechanics of blunt ballistic temporo-pariental head impact. PhD thesis (2008), Wayne State University, Detroit, Michigan.

[10] Rafaels K.A., Cutcliffe H.C., Salzar R.S., Davis M., Boggess B., Bush B., Harris R., Rountree M.S., Sanderson E., Campman S., Koch S., Dale Bass C.R., Injuries of the head from backface deformation of ballistic protective helmets under ballistic impact. J Forensic Sci. 60(1):219-25. doi: 10.1111/1556-4029.12570. Epub 2014 Jul 17. PMID: 25039407

[11] Freitas C.J., Mathis J.T., Scott N., Bigger R.P., and MacKiewicz J. "Dynamic response due to behind helmet blunt trauma measured with a human head surrogate," International Journal of Medical Sciences, 08 Mar 2014, 11(5):409-42, https://doi.org/10.7150/ijms.8079

[12] Merkle A.C., Wing I.D., Roberts J.C., et al. Human Surrogate Head Response to Dynamic Overpressure Loading in Protected and Unprotected Conditions. 26th Southern Biomedical Engineering Conference SBEC 2010, IFMBE Proceedings. 2010; 32: 22-25.

[13] Rodriguez-Millan M., Rubio I., Burpo F.J., Olmedo A.,. Loya J.A, Parker K.K., Miguélez M.H, Impact response of advance combat helmet pad systems, International Journal of Impact Engineering, Volume 181,023,104757, ISSN 0734-743X, https://doi.org/10.1016/j.ijimpeng.2023.104757.
[14] Rodriguez-Millan M., Rubio I., Burpo F.J., Tse K.M., Olmedo A., Loya J.A., Parker K.K., Miguélez M.H., Experimental and numerical analyses of ballistic resistance evaluation of combat helmet using Hybrid III headform, International Journal of Impact Engineering, Volume 179, 2023, 104653, ISSN 0734-743X, https://doi.org/10.1016/j.ijimpeng.2023.104653
[15] Pinnoji, P.K., Mahajan, P. Finite element modelling of helmeted head impact under frontal loading. Sadhana 32, 445–458 (2007). https://doi.org/10.1007/s12046-007-0034-6
[16] Palomar-Toledano, M.; Lozano-Mínguez, E.; Rodriguez-Millán, M.; Miguélez, MH.; Giner Maravilla, E. (01-1). Relevant factors in the design of composite ballistic helmets. Composite Structures. 201:49-61. https://doi.org/10.1016/j.compstruct.2018.05.076
[17] https://ciehub.info/spec/PD/FQ-PD-06-35A.pdf
[18] Moss W.C., King M.J., Blackman E.G.. Towards reducing impact-induced brain injury: lessons from a computational study of army and football helmet pads. Comput Methods Biomech Biomed Engin. 2014;17(11):1173-84. doi: 10.1080/10255842.2012.739162. Epub 2012 Dec 18. PMID: 23244512.
[19] Review of Department of Defense Test Protocols for Combat Helmets (2014); Committee on Review of Test Protocols Used by the Department of Defense to Test Combat Helmets. National Academies Press (US): Washington, DC, USA
[20] Li Y., Adanty K., Vakiel P., Ouellet S., Vette A.H., Raboud D., Dennison C.R. (2023) Review of mechanisms and research methods for blunt ballistic head injury. J Biomech Eng 145(1): 010801 (13 pages) Paper No: BIO-22–1088. https://doi.org/10.1115/1.40552 89
[21] Nsiampa, N., Coghe, F. Review of Literature: Behind Helmet Blunt Trauma Mechanisms. Hum Factors Mech Eng Def Saf 7, 6 (2023). https://doi.org/10.1007/s41314-023-00063-6
[22] Bass C., Bolduc M., and Waclawik S. (2002) Development of a Non-Penetrating, 9mm Ballistic Helmet Trauma Test Method. Proceedings of the Personal Armour Systems Symposium, pp. 18-22
[23] Sarron JC, Dannawi M, Faure A, Caillou JP, Da Cunha J, Robert R (2004) Dynamic effects of a 9 mm missile on cadaveric skull protected by aramid, polyethylene or aluminum plate: an experimental study. J Trauma. 2004 Aug;57(2):236-42; discussion 243. doi: 10.1097/01.ta.0000133575.48065.3f. PMID: 15345967
[24] NATO – AEP-103 Head injuries assessment of non-lethal projectiles. July 2021
[25] Raymond DE (2008) Biomechanics of blunt ballistic temporo-pariental head impact. PhD thesis, Wayne State University, Detroit, Michigan.
[26] Raymond D., Van Ee C., Crawford G., Bir C. (2009) Tolerance of the skull to blunt ballistic temporo-parietal impact. J Biomech. Nov 13;42(15):2479-85. doi: 10.1016/j.jbiomech.2009.07.018. Epub 2009 Aug 11. PMID: 19674749
[27] Nsiampa N., Coghe F., Modeling of Schuberth helmet under ballistic impact for head injury assessment, 34th International Symposium on Ballistics, May 2025
[28] Krishnan K., Rajan S.D., Belegundu A.D., (2008) A general optimization methodology for ballistic panel design. Paper presented at the Eng Opt 2008 conference, Rio de Janeiro, Brasil
[29] https://www.ansys.com/products/structures/ansys-ls-dyna
[30] Tan L.B., Chew F.S., Tse K.MM, Chye Tan V.B., Lee H.P.. Impact of complex blast waves on the human head: a computational study. Int J Numer Method Biomed Eng. 2014 Dec;30(12):1476-505. doi: 10.1002/cnm.2668. Epub 2014 Sep 17. PMID: 25132676.
[31] Deck C., Willinger R. Head injury prediction tool for protective systems optimisation. In 7th European LS-DYNA Conference, DYNAmore GmbH, Salzburg, Austria, May 14-15, 2009.
[32] Willinger R., Taleb L., Kopp C. Modal and temporal analysis of head mathematical models. J Neuro- trauma. 1995; 12: 743–754. https://doi.org/10.1089/neu.1995.12.743 PMID: 8683626
[33] Yoganandan N., Pintar F.A., Sances A., Walsh P.R., Ewing C.L., Thomas D.J., Snyder R.G., Biomechanics of skull fracture. J Neurotrauma 1995;12(4):659-668.
[34] Nahum A.M., Smith R., Ward C.C. Intracranial pressure dynamics during head impact, SAE Tech. Pap. 770922 (1977).
[35] Moss W. & King M. (2011). Impact Response of US Army and National Football League Helmet Pad Systems. 60. 10.2172/1021058.


https://doi.org/10.52202/081621-0013